Neutron News

ISSN: (Print) (Online) Journal homepage: https://www.tandfonline.com/loi/gnnw20

Quantum Effects of Neutron Scattering on Indistinguishable Particles

Erik B. Karlsson

To cite this article: Erik B. Karlsson (2023) Quantum Effects of Neutron Scattering on Indistinguishable Particles, Neutron News, 34:1, 16-19, DOI: 10.1080/10448632.2023.2166760

To link to this article: https://doi.org/10.1080/10448632.2023.2166760

OPEN ACCESS

Quantum Effects of Neutron Scattering on Indistinguishable Particles

Erik B. Karlsson
Department of Physics and Astronomy, Uppsala University, Uppsala, Sweden erik.karlsson@physics.uu.se

A recent paper by Matsumoto et. al [1] revitalizes the discussion of neutron scattering on indistinguishable particles, started in 2000 by Karlsson and Lovesey [2]. In a QENS measurement, Matsumoto et al. showed that the proton entanglement created in scattering on SiH_2 (deposited on Si-surfaces) changes the conditions for vibrational excitations of the SiH_2 "molecules"; the second scissor mode at 226 meV was strongly reduced compared to the first one at 113 meV. The present note will discuss the selection rules for vibrational excitations when the proton pairs are quantum entangled during scattering, and relate them to the reduced Compton cross-sections for such proton pairs, first discussed theoretically in [2].

It is well known that in the collision of two particles of the same kind, like in electron-electron scattering, their space and spin states become entangled, which leads to interference terms in the cross-section (see Schiff [3], Ch. 6). But the same is valid also for two or more identical particles of any kind which are interacting coherently with a neutron or an X-ray photon in scattering experiments (measurement-induced entanglement). In QNES as well as in Compton scattering, the coherence volume $V_{coh} = l_x \times l_y \times l_z$ contains more than one particle if the energy resolution (determining l_z) is high and the detector solid angles (determining l_x and l_y) are small enough.

For the simplest case of only *two* particles a and b within V_{coh}, the initial state of the scattering system can be taken as [[2],

$$\Psi_i = (1/\sqrt{2})\{\varphi(\mathbf{R}_{a1})\varphi(\mathbf{R}_{b2}) + (-1)^{Ji}\varphi(\mathbf{R}_{b1})\varphi(\mathbf{R}_{a2})\}\chi_M^{Ji}(a,b) \quad (1)$$

with particle a having equal amplitudes at sites $\mathbf{R}_{a1}$ and $\mathbf{R}_{a2}$ and similarly for particle b. The spins I_a and I_b of the two particles add up to quantum numbers J and M, described by the spin function $\chi_M^{Ji}(a,b)$.

In a *weak collision* with the neutrons (like in QENS), the protons suffer only a small recoil and remain essentially in their spatial positions, but the interaction can result in a spin-flip of one of the protons, changing J_i to J_f for the proton pair in the final state,

$$\Psi_f = (1/\sqrt{2})\{\varphi(\mathbf{R}_{a1})\varphi(\mathbf{R}_{b2}) + (-1)^{Jf}\varphi(\mathbf{R}_{b1})\varphi(\mathbf{R}_{a2})\}\chi_M^{Jf}(a,b) \quad (2)$$

In a *strong collision*, to be treated later, one of the particles recoils out of its original position and proceeds in the form of a plane wave $\mathbf{p}' = \mathbf{q} + \mathbf{p}$, where $\mathbf{p}$ is its initial momentum in its position in the molecule or crystal. For protons, this happens in the regime of Compton scattering for transferred momenta $q \gtrsim 20\,\text{Å}^{-1}$.

The matrix elements $< \Psi_f\, \Phi_{sc} | H_{op} | \Psi_i\, \Phi_g >$ for the excitation of vibrational states $\Phi_g \text{—>} \Phi_{sc}$ of SiH_2 in QENS experiments contain products of spatial integrals $\int d\mathbf{R}_i\, \varphi^*(\mathbf{R}_{ai})\varphi(\mathbf{R}_{bi})$ (which can all be taken as equal), spin factors $[1 + (-1)^{Ji}] \times [1 + (-1)^{Jf}]$ from Equations (1) and (2), a factor $(-1)^{\Delta Jvib} = (-1^{(JSC - JG)})$ from the vibrational state transition elements and the spin factor

$(-1)^{\Delta Jn}$ for the neutron interaction operator H_{op}. The selection rule is $J_i + J_G = J_f + J_{SC} + \Delta J_n$ or

$J_i - J_f = \Delta J_{vib} + \Delta J_n$, with $\Delta J_n = 1$ for spin-flip and $\Delta J_n = 0$ for non-spin-flip, leading to

$$(1/4)\left[1+(-1)^{J_f}\right]\left[1+(-1)^{J_i}\right]\sigma_{coh} \text{ for } J_f = J_i \quad (3a)$$

$$(1/4)\left[1+(-1)^{J_f}\right]\left[1+(-1)^{J_i}\right]\sigma_{incoh} \text{ for } J_f = J_i \pm 1 \quad (3b)$$

The cross-sections for the transitions $\Psi_G \rightarrow \Psi_{1SC}$ ($\Delta J_{vib} = +1$) and $\Psi_G \rightarrow \Psi_{2SC}$ ($\Delta J_{vib} = 0$) with $N=2$ are summarized in Table 1.

Therefore, the transition from the ground state Ψ_G (J=0) to Ψ_{1SC} (J=1) should be allowed and exhibit the incoherent cross-section $\sigma_{H,incoh}$, while the Ψ_G (J=0) to Ψ_{2SC} (J=0) transition should show only the small coherent cross-section $\sigma_{H,coh}$, as also stated by Matsumoto et al. [1] (but for distinguishable protons be determined by $\sigma_{H,tot}$). The measured scattering from the protons in the Ψ_G (J=0) to Ψ_{2SC} (J=0)

Table 1.

Transition	ΔJ_{vib}	J_i	J_f	ΔJ_n	Cross-section
$\Psi_G \rightarrow \Psi_{1SC}$	1	0	0	–1	σ_{incoh}
	1	0	1	(-2)	0
	1	1	0	0	0
	1	1	1	–1	0
$\Psi_G \rightarrow \Psi_{2SC}$	0	0	0	0	σ_{coh}
	0	0	1	–1	0
	0	1	0	–1	0
	0	1	1	0	0

transition is indeed much lower than expected for distinguishable protons (see [1], Figure 2c, here reproduced in the left hand panel of Figure 1), but actually *not as low* as $\sigma_{H,coh}$ (cf. right hand panel of Figure 1).

The fact that the observed transition $\Psi_G \rightarrow \Psi_{2SC}$ is stronger than expected for $\sigma = \sigma_{coh}$ is probably a consequence of multi-proton involvement. Table 1 is valid for two entangled particles, but Figure 2d of the Matsumoto et al. paper [1] shows Fourier transformed S(Q, ω) spectra which indicate involvement of protons up to 6 Å distance from each other, corresponding to at least two of the SiH_2 terminations in their Figure 1a, i.e. at least *four* identical particles within V_{coh}.

The situation with *several* indistinguishable particles within V_{coh} has been studied in neutron Compton scattering on protons (and deuterons) in metallic hydrides. Before returning to the SiH_2 data, it is therefore appropriate to look back at the so-called "hydrogen anomaly problem", discussed in the early 2000s. Hydrogen anomalies were first observed by Chatzidimitriou-Dreismann et al. in water [4] and by Karlsson et al. in metal hydrides [5] and later in many other hydrogen-containing substances (for a review, see [6]).

With two identical particles *a* and *b* within V_{coh} in Compton scattering, one of them recoils with momentum $\mathbf{p}' = \mathbf{q} + \mathbf{p}$ (where $\mathbf{p}$ is its initial momentum) and is expelled in the form of a plane wave $\exp(i\mathbf{p}'\cdot\mathbf{R}_{a1})$, while the other one (*b* or *a*) remains at its site, $\varphi(\mathbf{R}_{b2})$. As pointed out by Karlsson in 2012 [7], exchange symmetry then requires that the final state wavefunction of the entangled pair must be described by two interfering waves $\Psi_{f,\,Compt}(1)$ and $\Psi_{f,\,Compt}(2)$ with opposite phase factors,

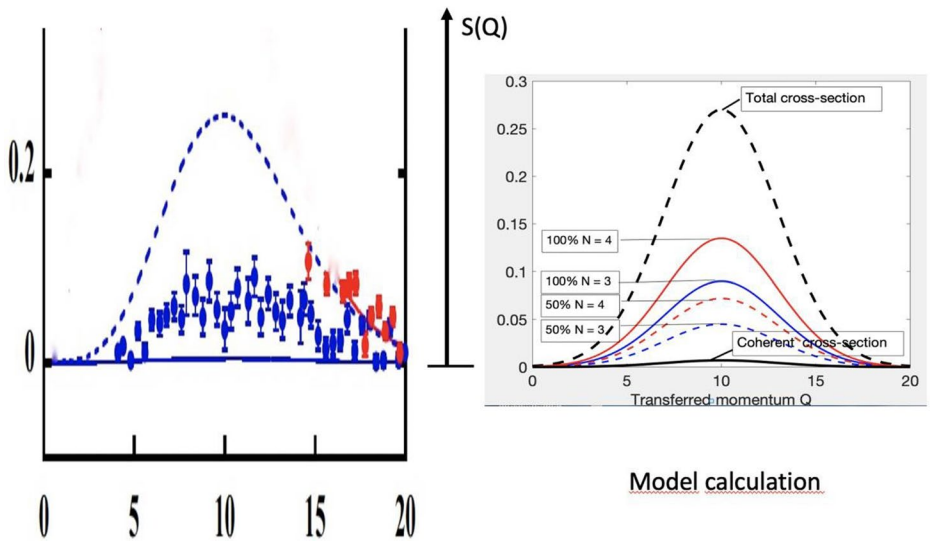

Figure 1. (Left panel) Excerpt from Figure 2c of Ref. [1]. Dashed blue line: expected proton intensity for indistinguishable protons; blue symbols: measured intensities. (Right panel) Full blue line: $N=3$ identical protons seen by the neutron with 100% probability (dashed blue line with 50%). Full red line: $N=4$ protons seen with 100% probability (dashed red line with 50%).

$$\psi_{f,\mathrm{Compt}}(1) = \\ = (1/2\sqrt{2})\{\exp(i\mathbf{p}'\cdot\mathbf{R}_{a1})\varphi(\mathbf{R}_{b2}) + (-1)^{J'}\exp(i\mathbf{p}'\cdot\mathbf{R}_{a2})\varphi(\mathbf{R}_{b1}) + \\ + \varphi(\mathbf{R}_{a1})\exp(i\mathbf{p}'\cdot\mathbf{R}_{b2}) + (-1)^{J'}\varphi(\mathbf{R}_{a2})\exp(i\mathbf{p}'\cdot\mathbf{R}_{b1})\}\chi^{J'}_{M'}((a,b) \quad (4a)$$

$$\psi_{f,\mathrm{Compt}}(2) = \\ = (1/2\sqrt{2})\{\exp(i\mathbf{p}'\cdot\mathbf{R}_{a1})\varphi(\mathbf{R}_{b2}) - (-1)^{J'}\exp(i\mathbf{p}'\cdot\mathbf{R}_{a2})\varphi(\mathbf{R}_{b1}) + \\ + \varphi(\mathbf{R}_{a1})\exp(i\mathbf{p}'\cdot\mathbf{R}_{b2}) - (-1)^{J'}\varphi(\mathbf{R}_{a2})\exp(i\mathbf{p}'\cdot\mathbf{R}_{b1})\}\chi^{J'}_{M'}(a,b) \quad (4b)$$

It was shown in [7] that a neutron-proton interaction in the form $O_n = b_n[\exp(i\,\mathbf{q}\cdot\mathbf{R}_a) + \exp(i\,\mathbf{q}\cdot\mathbf{R}_b)]$ leads to the following spatial scattering matrix elements

$$<\psi_{f,\mathrm{Compt}}(1)|O_n|\psi_i>_{spat} = (1/4)\{1+(-1)^{I+J'}\exp(i\mathbf{p}\cdot\mathbf{d})\}K(\mathbf{p}) \quad (5a)$$

$$<\psi_{f,\mathrm{Compt}}(2)|O_n|\psi_i>_{spat} = (1/4)\{1-(-1)^{I+J'}\exp(i\mathbf{p}\cdot\mathbf{d})\}K(\mathbf{p}) \quad (5b)$$

where $\mathbf{d} = \mathbf{R}_1 - \mathbf{R}_2$ and $K(\mathbf{p})$ is the so-called Compton integral $K(\mathbf{p}) = \int d\mathbf{R}\exp(-i\mathbf{p}\cdot\mathbf{d})\varphi(\mathbf{R})$ which results in a modified cross section σ_{eff} per nucleus as compared to single particle scattering σ_{sp},

$$\sigma_{eff} = (1/4)\{[1+<\exp(i\mathbf{p}\cdot\mathbf{d})>]^2 + [1-<\exp(i\mathbf{p}\cdot\mathbf{d})>]^2\}\sigma_{sp} = \\ = (1/2)(1+<\exp(i\mathbf{p}\cdot\mathbf{d})>^2)\sigma_{sp} \quad (6)$$

It was also first understood in [7] that the reason for the hydrogen anomalies in water, hydrocarbons and metal hydrides is that the protons are simultaneously in all motional states **p** allowed by their zero-point distributions n(**p**), which have intrinsic spreads of 3 – 4 Å^{-1}. For each scattering event the factor exp(i**p** • **d**) in (5) must therefore be *integrated over the n*(**p**) *distribution*,

$$<\exp(i\mathbf{p}\cdot\mathbf{d})> = \int n(\mathbf{p})\exp(i\mathbf{p}\cdot\mathbf{d})d\mathbf{p} \quad (7)$$

For $\mathbf{p}=0$ and for $\mathbf{p} \perp \mathbf{d}$, $\exp(i\mathbf{p}\cdot\mathbf{d}) = 1$ Equation (6) gives the standard result $\sigma_{eff} = \sigma_{sp}$, but for $\mathbf{p} \parallel \mathbf{d}$ the integral in Equation (6) is strongly reduced when the distribution n(**p**) contains several oscillations in the exponential. With inter-particle distances d = 1 – 3 Å, the $\mathbf{p} \parallel \mathbf{d}$ integral is effectively zero, which leads to reduced cross-sections with $\sigma_{eff} = (5/8)\sigma_{sp}$. For scattering on YH_2 a more refined calculation, taking into account the actual scattering geometry, led to $\sigma_{eff} = 0.56\,\sigma_{sp}$ [8].

In physical terms, the cross-section reduction is caused by destructive interference when partial waves with a phase distribution covering a large fraction of 2π are scattered from two (or a few) near-lying centers. As mentioned in Sections 7.2 and 8.4 of Ref. [6], similar reductions have also been observed in high energy electron scattering experiments where only few particles are located within V_{coh} (which falls in the 10^5 Å^3 range or below; in gaseous H_2 at NTP there is on the average one molecule per 38×10^3 Å^3). Cooper et al. [9] scattered electrons on 50–50% gaseous H_2-D_2 mixtures and found a cross-section reduction by 39% for H in H_2 while HD-molecules (distinguishable particles) showed expected values for H (further analyzed by Vos and Went in [10]) For a recent review of scattering on zero-point states, see Ref. [11].

The extension to more than two identical particles within V_{coh} was first discussed for $N=3$. It was shown in [7] that entanglement then appears only pairwise, which decreases the cross-section anomaly by 2/3 for $N=3$; and by $2/N$ when N is further increased (a consequence of the "entanglement monogamy" theorem [12] in quantum information theory). Figure 2 below (from Ref. [13]) illustrates the dependence on coherence volume V_{coh} for the effective neutron H-cross-sections measured in metallic hydrides with different energy resolutions and detector arrangements. The coherence length $(l_{coh})_{\parallel}$ was changed by operating with Rh-103 foil energy selection instead of Au-197 and $(l_{coh})_{\perp}$ was changed by varying the detector geometry. $V_{coh} = 6$ Å^3 in Figure 2 corresponds to $N=2$ and $V_{coh} = 35$ Å^3 to $N\approx10$. For $N<2$, only part of the events showed reduced cross-sections, because some events are scattering on single protons. Similar coherence volume dependencies were found in the electron scattering experiments on CH_4 by Vos et al. [14] were the

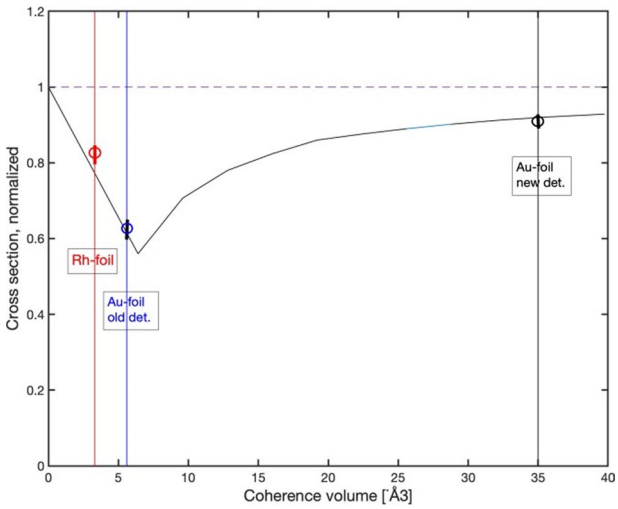

Figure 2. Cross-section reductions for coherence volumes including less than one proton pair (red), about one proton pair (blue) and about 5 proton pairs in neutron Compton scattering. Reproduced from Ref. [13].

anomaly in the hydrogen cross-section decreased with increasing electron energy (giving higher ΔE/E and $(l_{coh})_{\parallel}$): 10% reduction for 2 keV electron energy, 3% for 3 keV and 2% for 6 keV).

The exact proportions of $N=2$, $N=3$, $N=4$, etc. probabilities for protons seen by each neutron in the QENS experiment performed by Matsumoto et al. [1] cannot easily be estimated, but the consequences of deviation from the $N=2$ assumption for the proton entanglement is here modelled in right hand panel of Figure 1.

For $N=3$, the entanglement effect is expected to be 2/3 of that for $N=2$. The $N=3$ coverage (on two protons in one SiH_2 termination and one in another one) is not easily compatible with the simultaneous vibrational excitation of one pair of protons, but coverage of two pairs of protons belonging to two different SiH_2 terminations is possible in principle ($N=4$). The dashed red line in the model calculation (Figure 1) shows what is expected from a 50% coverage of four equivalent protons and seems to be compatible with the experimental data. For comparison, the expected S(Q) distribution for a single SiH_2 termination ($N=2$), determined by the $\sigma_{H,\,coh}$ cross-section according to Table 1, is included in the right-hand panel of Figure 2.

However, the question arises whether protons within two different SiH_2 molecules can be considered indistinguishable (like the protons in metallic hydrides referred to in Figure 1). If not, scattering will involve two proton pairs (*a,b* and *c,d*) having entanglement effects and four others (*a,c, a,d*, *b,c* and *b,d*) having normal cross-sections, which also gives ½ reduction of the $N=2$ effect.

With sufficient energy resolution, similar effects should also be expected in QENS experiments on H_2O, but existing data [15] do not seem to allow it. Generic effects of quantum entanglement created in scattering of different particles were discussed in [13] and consequences of the initial n-p entanglement in neutron scattering for the energy balance of inelastic transitions in [16].

References

1. T. Matsumoto et al., *Phys. Rev. B.* **103** (24), 245401 (2021). doi:10.1103/PhysRevB.103.245401
2. E. B. Karlsson, and S. W. Lovesey, *Phys. Rev. A.* **61** (6), 062714 (2000).
3. L. I. Schiff, *Quantum Mechanics* (McGraw-Hill, New York 1955). Ch. 9.
4. C. A. Chatzidimitriou-Dreismann et al., *Phys. Rev. Lett.* **79** (15), 2839 (1997).
5. E. B. Karlsson et al., *Europhys. Lett.* **46** (5), 617 (1999).
6. E. B. Karlsson, *Phys. Scr.* **93** (3), 035801 (2018). doi:10.1088/1402-4896/aa9b6e
7. E. B. Karlsson, *Int. J. Quantum Chem.* **112** (2), 587 (2012). doi:10.1002/qua.23023
8. E. B. Karlsson et al., *Meas. Sci. Technol.* **28** (7), 079501 (2017). doi:10.1088/0957-0233/27/8/085501
9. M. J. Cooper, A. P. Hitchcock, and C. A. Chatzidimitriou-Dreismann, *Phys. Rev, Lett.* **100**, 043204 (2008).
10. M. Vos, and M. R. Went, *J. Phys. B: At. Mol. Opt. Phys.* **42** (6), 065204 (2009).
11. E. B. Karlsson, *Trends Phys. Chem.* **22**, 1 (2022).
12. M. Koashi, and A. Winter, *Phys. Rev. A.* **69** (2), 022309 (2004).
13. E. B. Karlsson, *Phys. Scr.* **96** (2), 025104 (2021). doi:10.1088/1402-4896/abd0be
14. M. Vos et al., *J. Phys. B: At. Mol. Opt. Phys.* **41** (13), 135204 (2008).
15. ISIS Experiment RB12519 (Rutherford-Appleton Laboratory, UK).
16. E. B. Karlsson, *Phys. Scr.* **95** (2), 025003 (2020). doi:10.1088/1402-4896/ab499c